

**An Enzymatic Study of the Role of Tyr415 in Native Catalase HPII
Using the UAA Mutants: 3-Cl-Tyr415 and 3-Br-Tyr415**

Author: Natasha Smith

Co-Investigators: Reid Kinser, Megan Iverson, and Gavin Rodgers

Oregon State University

3-11-16

ABSTRACT:

Catalase HPII from *Escherichia coli*, is a mono-functional catalase responsible for preventing the formation of reactive oxygen species in the cell. Its active site is representative of most mono-functional catalases, making it a good model for mechanistic studies. The role of the heme-binding tyrosine was investigated by replacing Tyr415 with two types of unnatural amino acids: 3-chlorotyrosine and 3-bromotyrosine. The designed mutants were expressed and purified in large quantities alongside the native catalase with an approximate 67% purity for 3-Cl-Tyr-415 and 78.5% for 3-Br-Tyr-415. In addition, the translational machinery was shown to be high fidelity. Quantitative kinetic assays were performed on the native catalase and 3-Cl-Tyr415 and 3-Br-Tyr415 mutants. Electronic properties were unable to be investigated due to issues with purity, but the mutants were shown to have comparable activity levels to the native. In addition, they demonstrated higher turnover numbers and lower specificity constants as compared to native. Lastly, the mutants denatured at around the same temperature as the native but showed greater constancy in terms of activity over lower temperatures. Successful incorporation of a mutant at Tyr415 has never been done before in literature and possesses serious implications for the ability of scientists to understand the catalytic role of the tyrosine ligand in monofunctional catalases.

INTRODUCTION:

Catalases are a class of enzymes responsible for the breakdown of hydrogen peroxide in cells.¹ Hydrogen peroxide is a natural byproduct of cellular processes such as fatty acid β -oxidation, but can generate reactive oxygen species if not properly maintained. Due to their essential role in maintaining a healthy intracellular environment, catalases are found in nearly all living organisms exposed to oxygen.² Despite having been studied for nearly 200 years, their mechanism is still not fully understood.³ In this work, we investigate the catalytic efficiency and stability of *Escherichia coli* HPII catalase with Tyr415 replaced by the unnatural amino acids 3-chlorotyrosine and 3-bromotyrosine. Unnatural amino acids, or UAA's, provide a unique opportunity to study protein mechanics by introducing new functional groups beyond those provided by nature's toolbox.

Escherichia coli's HPII catalase provides an excellent model for many other mono-functional heme-binding catalases, including mammalian forms like the human erythrocyte catalase.⁴ All of these mono-functional catalases show a high degree of structural similarity in the catalase fold containing the active site. In particular, the heme iron is buried deep in the protein and is coordinated to a proximal tyrosine (Tyr415 in HPII).^{4,5} Discoveries into the mechanism of HPII will thus yield important insights into the functionality of many other catalases.

A better understanding of mono-functional catalases' mechanisms are expected to lead to important new medical and biotechnological applications.⁵ For example, individuals with AIDS are particularly susceptible to a pathogenic bacteria known as *Mycobacterium avium*.⁶ The bacterium's resistance to isoniazid, a powerful antituberculosis drug is thought to be linked to the presence of catalase HPII.⁶ There are also interesting correlations between catalase and healthy aging.⁵ In a highly cited study,

mice that overexpressed a mitochondrial catalase showed increases in both health and lifespan.⁵ Conversely, there are problems associated with underexpression of catalase. Some humans have a mutation that results in non-functional catalase and a condition known as acatalesemia.³ It causes the individual to be more susceptible to infections from H₂O₂ producing bacteria like streptococci and pneumococci.³ Acatalesemia has also been linked to damage of the insulin-producing β-cells of the pancreas resulting in diabetes mellitus type I, a severe autoimmune disorder.³

In order to prevent cytotoxic effects such as these, catalases act to break hydrogen peroxide into harmless oxygen and water before the hydrogen peroxide has the chance to generate radicals (Equation 1).¹



Catalase HPII is a monofunctional tetramer with a heme as a prosthetic group in each subunit.¹ The heme iron is covalently bound to catalase through the hydroxyl of Tyr415.¹ There are two primary channels involved in each active site.⁷ The main channel, where reactant enters, runs perpendicular to the heme plane and is on the distal side of the heme with respect to Tyr415 (Figure 1c).⁷ The shorter lateral channel, through which products exit, runs parallel with the plane of the heme and extends to the left of Figure 1d.⁷

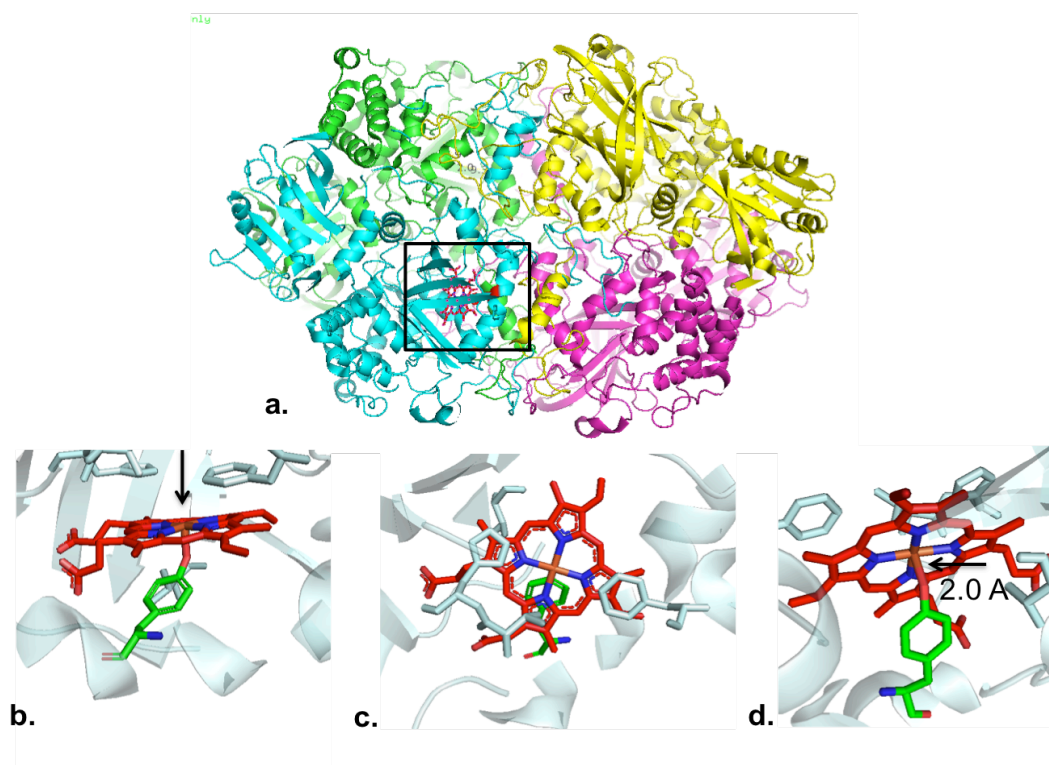
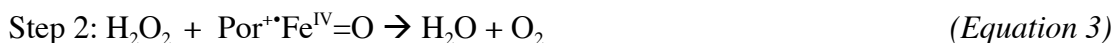


Figure 1: The structure of catalase HPII as determined by x-ray crystallography: (a) the tetramer with the active site inside the box, (b) a lateral view of Tyr415 covalently bonded to the heme in the active site (main channel indicated by arrow), (c) a superior view of the heme as it appears looking through the main channel, and (d) an inferior view of the Tyr415-heme interaction. Note the bond distance between the iron and tyrosine oxygen in (d) is 2.0 Å and indicative of a covalent bond.

In *E. coli*, catalase HPII functions via a two-step mechanism.¹



In Step 1, hydrogen peroxide reacts with the iron-porphyrin (III) complex.⁸ When this occurs the oxygen, previously of peroxide, double bonds to the iron atom. This oxidation generates the Fe^{IV} state, hereafter referred to as Compound I.⁸ In this intermediate state, there is a pair of delocalized electrons on the oxy-ferryl group and a single delocalized electron in the porphyrin ring system.⁹ A water molecule leaves via the lateral channel.⁷

In Step 2, another peroxide molecule enters the active site via the main channel and reacts with Compound I.^{7,8} Two electrons are transferred from the peroxide molecule to Compound I during the second step of the enzymatic reaction, reducing the molecule to its original form, and releasing a water and oxygen molecule.⁹

According to Obinger *et al.*, Step 1 is the rate-limiting step with a rate constant of $1.3 \times 10^6 \text{ M}^{-1}\text{s}^{-1}$.¹ Step 2 is faster with a rate constant of $1.8 \times 10^6 \text{ M}^{-1}\text{s}^{-1}$.¹ Tyrosine 415 plays a crucial role in modulating heme iron reactivity by stabilizing higher oxidation states.¹⁰ Historically, attempts to mutate the Tyr 415 residue to histidine have not been successful.¹¹ No protein was accumulated.¹¹ We predict that modification of the electron density in the aromatic ring of Tyr415 will not only produce active protein, but will alter the efficiency of each step by influencing the stability of Compound I. For example, if an electron-withdrawing group is attached to the aromatic ring of the tyrosine, electron density would be withdrawn from the oxygen-iron covalent bond via the inductive effect. Theoretically, this would serve to stabilize the oxidized Compound I over the reduced Fe^{III} heme. Since the rate-limiting step is the formation of Compound I, this could increase the rate of the overall reaction. Of course, by stabilizing Compound I we also run the risk of slowing the rate of Step 2. To test this, we will incorporate two unnatural amino acids (UAA's) into the Tyr415 position that have electron-withdrawing effects on the aromatic ring. The UAA's we have selected are 3-chloro-tyrosine and 3-bromo-tyrosine, respectively (Figure 2). These UAA's were selected based on their electronegativity, the comparable steric effects they will have on the system, and their structural similarity to the wild type residue.

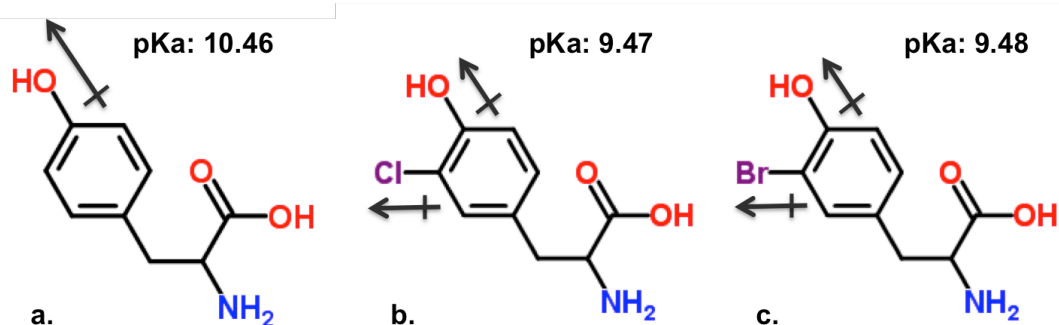


Figure 2: The structures of (a) Tyr, (b) 3-Cl-Tyr, and (c) 3-Br-Tyr. Note the higher electron density of the hydroxyl in (a) over (b) and (c). The halogens serve to reduce the net electronegativity of the hydroxyl group via the inductive effect and to lower the pKa of the hydroxyl group.

The inductive effect of the halogens can be observed by noting the lower pKa's of the hydroxyl group. In fact, the pKa's are nearly 10 times lower in 3-chloro-tyrosine and 3-bromo-tyrosine. Our hypothesis that this will serve to stabilize Compound 1 and speed the rate of reaction is supported by a similar experiment done in myoglobin. The structure of the active site is different, but still involves a tyrosine as an electron donor. In this study by Yu et al., Tyr33 was replaced by UAA's with electron withdrawing groups.¹² They found a strong relationship between lowered pKa of the tyrosine and increased catalytic rate.¹²

By only slightly altering the structure of Tyr415, we also predict the protein will still be able to fold properly. Analysis of the electron density surrounding the tyrosine indicates there is room for a halogen on the third carbon of the aromatic ring (Figure 3).

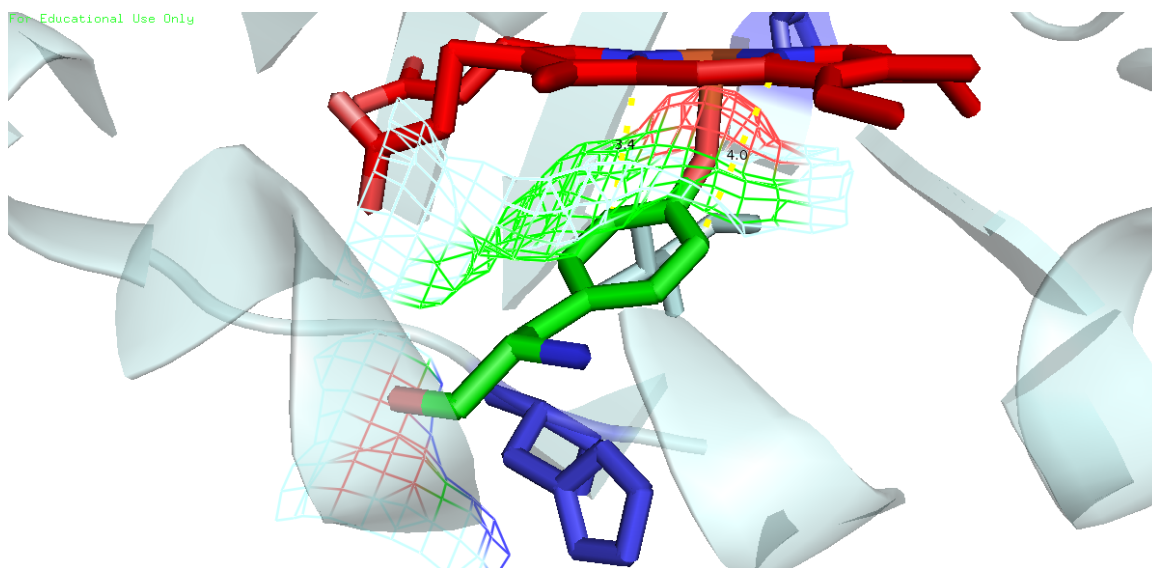


Figure 3: An electron density distribution of the catalytic Tyrosine 415. The figure indicates there is room to incorporate a halogen on the third carbon of the tyrosine ring without causing a major shift in adjacent structures. Distances between the third carbon of the aromatic ring and the closest atom on the porphyrin ring are displayed. The

shortest distance of 3.4 Å easily accommodates a chlorine ($r=0.97$ Å) and Bromine ($r=1.12$ Å). Literature also states the importance of His 392 (blue) being able to form a covalent bond with the beta carbon of tyrosine.¹¹ The halogen should not spatially interfere with this interaction either.

There are several aims for this study. The first is to determine if catalase will fold properly and have catalytic activity when Tyr 415 is replaced with 3-chloro-tyrosine or 3-bromo-tyrosine. Secondly, does the presence of an electron withdrawing group speed the rate of reaction over the native enzyme? If it does, we can infer that stabilization of Compound I increased the rate of Step I more than it decreased the rate of Step 2. And lastly, if the rate does not increase over that of the native enzyme, how does it change with respect to increasing electronegativity of the substituent? We hypothesize that 3-chloro-tyrosine will have a greater inductive effect and will correspondingly have a faster catalytic rate than 3-bromo-tyrosine.

EXPERIMENTAL

Expression:

The *Escherichia coli* DH10B cells used for protein expression contained a pBAD plasmid encoding the His-tagged catalase gene, ampicillin resistance, a β -lactamase gene, and an arabinose promoter system.¹³ In addition, cells contained a pDULE plasmid encoding the necessary translational machinery and a protein for spectinomycin resistance (Figure 4).¹³ Cells were diluted 1:100 in 75 mL of autoinduction media in a flask. See Supplemental Table 1 for specifics on preparing autoinduction media. Eight cultures were grown: native catalase HPII, 3-Cl-Tyr-415 catalase, 3-Br-Tyr-415 catalase, 3-Cl-Tyr-415 catalase with no UAA added, 3-Cl-Tyr-206, 3-Cl-Tyr-206 with no UAA added, 3-Br-Tyr-206, and an sfGFP. The UAA's, UAA translational machinery, and spectinomycin were added to each of the mutant cultures. The cultures grown without UAA were controls to test the fidelity of the translational machinery. Since the translational machinery is designed to incorporate the UAA at a TAG codon, the absence of a UAA should result in a truncated protein. The translational machinery can incorporate both 3-chloro-tyrosine and 3-bromo-tyrosine, so only one control was needed. 3-Cl-Tyr-206 and 3-Br-Tyr-206 were grown as controls in case no protein accumulated. If no 415 mutants accumulated, but 206 mutants did then problems with the translational machinery could be eliminated. This 206 set also had a minus UAA control. Lastly, an sfGFP control was grown to compare levels of expression. The cultures were incubated on a rocker at 37°C for 48 hours.

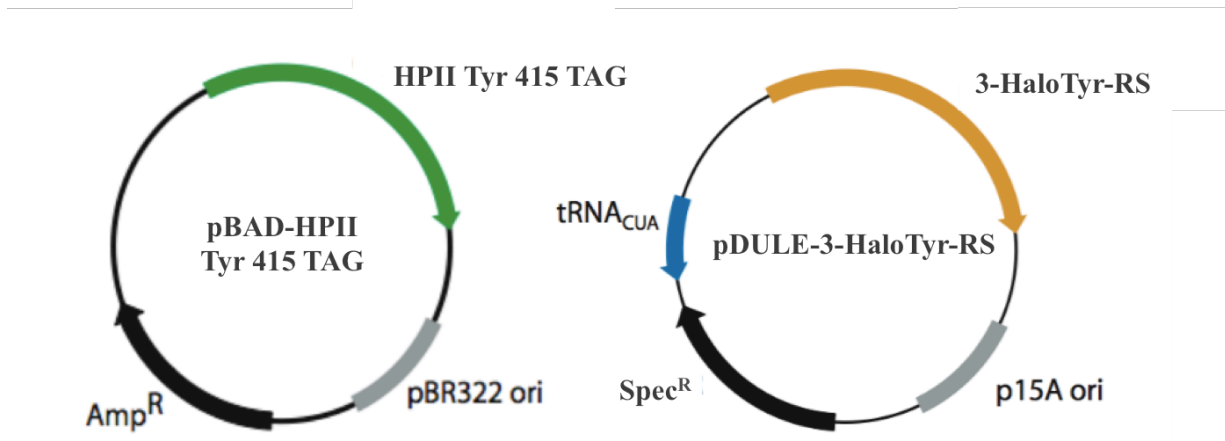


Figure 4: The plasmid vectors for the catalase gene (left) and translational machinery (right).¹³

After incubation, 250 μ L of each culture was extracted, centrifuged at 4000 RCF for 7 minutes, and resuspended in 50 mL water for the purpose of a crude SDS-PAGE gel. The remaining cultures were centrifuged for 10 minutes at 7000 ref. Each cell pellet was stored at -80°C . Optical densities were measured at 600 nm using a UV-Vis spectrophotometer.

Purification of Protein:

For purification, each cell pellet was re-suspended in 10 mL of 1X Talon equilibration buffer and processed in the microfluidizer. See Supplemental Table 2 for specifics on all buffer solutions. The resulting lysates were centrifuged at 15,000 rpm for 20 minutes at 4°C . Next, the cleared lysates were transferred to sterile tubes where 600 μ L of 50% Talon resin slurry was added. Each sample was placed on the rocker for 20 minutes at 4°C . During this time, the His-tagged catalase bound to the Talon resin. The supernatant was discarded and a series of washes were performed to rinse away all other proteins. The three washes consisted of adding 30 mL of Talon equilibration buffer, rocking for 10 minutes at 4°C , and centrifuging at 700 g for 5 minutes.

After washing, the majority of the supernatant was discarded and the remaining contents were transferred to a gravity flow column primed with equilibration buffer. The resin was allowed to settle to the bottom of the column before the excess buffer was drained. The protein was eluted in four 500 μ L fractions using elution buffer and stored in the 4°C fridge.

Protein Concentration Check:

A Bradford assay was performed on each fraction and the absorbance at 595 nm was compared to a standard curve to determine concentration. Each sample was prepared with

1 mL of Bradford reagent and 20 μL of protein. The standards were prepared with 1 mL of Bradford reagent and 20 μL of BSA at a range of 0-2000 $\mu\text{g}/\text{mL}$ (Figure S1).

Protein Purity Check:

To determine protein purity, SDS-PAGE of crude and purified protein was run at 200 V. A 7% acrylamide resolving gel and 4% acrylamide stacking gel with discontinuous Laemmli buffer system was used. The following volumes were added: 5 μL ladder, 10 μL sfGFP, and 20 μL of all remaining samples. Proteins were visualized using Coomassie Brilliant Blue Dye.

Kinetic Assays:

Qualitative:

A qualitative analysis of catalase activity was performed at 20 $^{\circ}\text{C}$ for 5 minutes. This was done by adding 1 μL of purified protein to 200 μL of 3% H_2O_2 . The presence of bubbles indicates the enzyme was active and producing oxygen gas.

Quantitative:

Quantitative assays were performed with a Vernier Pressure Sensor Probe to measure the rate of oxygen production. 1.25 μg of protein in 5 μL of Elution Buffer (Table S2) was added to varying concentrations of H_2O_2 and the initial velocity of each trial was plotted as a function of substrate concentration. Concentrations of H_2O_2 ranged from 0.5% to 3.0% in steps of 0.5%. The point at which the initial velocity stopped changing despite increasing substrate concentration was determined to be v_{max} . The ideal gas law was used to convert pressure to moles of hydrogen peroxide consumed. Assays were performed at 22 $^{\circ}\text{C}$ and at a volume of 9.1 mL. The Michaelis constant, K_m , is equal to the H_2O_2 concentration at $v_{\text{max}}/2$. The turnover number, k_{cat} , was found by the following equation:

$$k_{\text{cat}} = v_{\text{max}}/[\text{E}] \quad (\text{Equation 4})$$

Heat Denaturation Study:

To assess how tightly the heme group was bound to Tyr 415 and if this bond has any effect on the stability of the protein, a heat denaturation study was performed. Samples were heated for 10 minutes at the following temperatures: 22.0, 60.0, 64.0, 72.6, and 80.0 $^{\circ}\text{C}$. After heating, the samples were returned to ice to ensure no further denaturation would occur. Activity of each sample was determined by measuring the rate of oxygen production with a Vernier Pressure Probe for 100s. Assays were prepared by adding 1.25 μg of protein to 500 μL of a 2.0% H_2O_2 buffer solution. The initial velocity (15-55 seconds) was plotted as a function of temperature and the results analyzed.

RESULTS AND DISCUSSION:

E. coli cultures were prepared according to the methods described above and grew to the following optical densities. The mass of the cell pellet harvested and protein purified from each culture is also listed. We would expect the sfGFP to have the highest optical density, followed by the native, and then the rest of the cultures. The results support this. sfGFP has the highest optical density at 7.862, indicating the *E. coli* cells were viable and able to take up genetic material from the environment. The native optical density is almost as high as the sfGFP indicating the cells were fairly efficient at taking up the pBAD plasmids. All other remaining samples had optical densities within the desired range of 4.00 - 7.00 indicating cells had grown to a sufficient population for protein expression. There does not appear to be a clear trend between optical density and amount of purified protein. However, the optical density and pellet mass are related as would be expected.

Table 1: Optical density (600nm), cell pellet masses, and purified protein yield for each culture grown. All cultures grew to a sufficient population to express protein.

	Optical Density	Pellet Mass (g)	Protein purified (mg/L)
Native	7.459	0.83	11.77
sfGFP	7.862	0.93	NA
3-Cl-Tyr415	6.260	1.35	15.20
3-Br-Tyr415	6.627	1.28	36.77
415 +pDULE -UAA	5.586	1.47	9.87
3-Cl-Tyr206	6.884	1.46	11.84
3-Br-Tyr206	6.185	1.35	8.98
206 +pDULE -UAA	6.585	1.70	13.22

To assess purity, an SDS-PAGE was run on the most concentrated crude and purified samples (Figure 5). The crude gel was run to ascertain if a band was present at 84.2 kDa in the native, 3-Cl-Tyr-415, 3-Br-Tyr-415, 3-Cl-Tyr-206, and 3-Cl-Tyr-206 before proceeding to purification. This would indicate catalase had been produced. There should also be a visible band at 27 kDa for sfGFP. The results supported these criteria (Figure 5a). The band for sfGFP was not visible, because it had not yet separated on the gel.

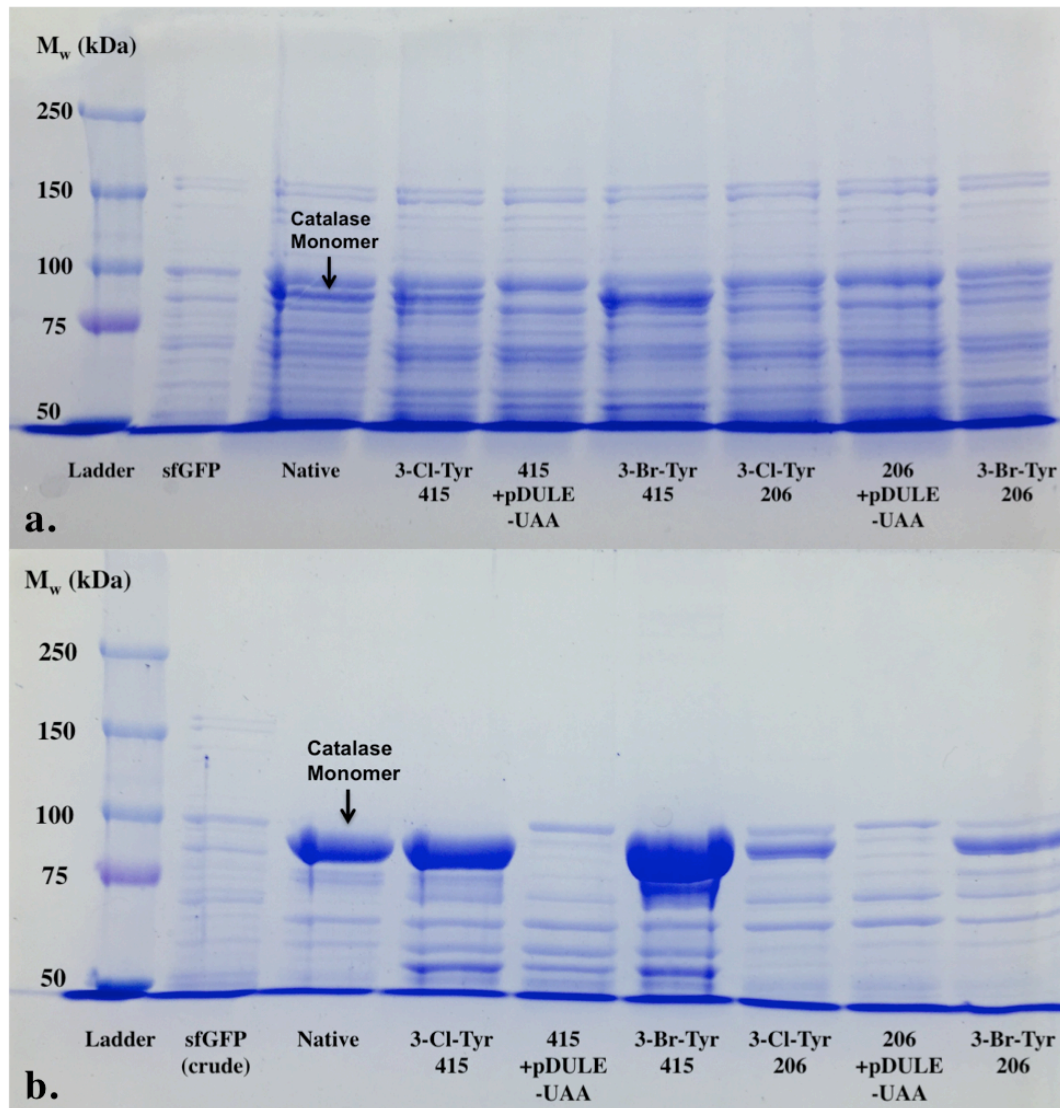


Figure 5: An SDS-PAGE gel comparing crude (a) and purified (b) cell lysates. A band for catalase at 84.2 kDa can be observed in the crude gel. The pure gel shows strong bands at 84.2 kDa for the Native, 3-Cl-Tyr-415, and 3-Br-Tyr-415 as expected. A weaker catalase band can also be observed in the 206 mutants indicating the translational machinery is capable of inserting into multiple sites. The $-UAA$ controls show no band at 84.2 kDa indicating the translational machinery is high fidelity. This demonstrates the desired mutants were successfully made.

After purification, another SDS-PAGE gel was run to assess the purity of the proteins, determine the fidelity of the transcriptional machinery, and obtain a qualitative read on the quantity of protein produced. Ideally, strong bands should be present at 84.2 kDa for the Native, 3-Cl-Tyr-415, 3-Br-Tyr-415, 3-Cl-Tyr-206, and 3-Br-Tyr-206. A high purity sample would show only a single band at 84.2 kDa. In fact, strong bands are present at 84.2 kDa (Figure 5b). Interestingly, the 415 mutants have even stronger bands than the native catalase. This could indicate the presence of the electron withdrawing

halogen aids in the rate of protein folding, or it could simply be an artifact of how the fractions were collected. Further testing would need to be done to support this hypothesis. The strong bands also indicate the mutants are highly soluble in the buffer. The 206 mutants show considerably less protein than the native and 415 mutants. This is not a surprise. The purpose of these controls was to show that the translational machinery is capable of inserting the UAA's into a different site. Site 206 is normally a phenylalanine important in gating of the main channel, so it would be expected that replacing a phenylalanine with a larger tyrosine could disrupt protein folding and result in less product.¹⁴

The sfGFP was not purified and can be expected to show multiple bands, but there should be a strong one around 27 kDa. While the gel does show multiple bands, it is not possible to tell if GFP is present at 27 kDa, because the low molecular weight proteins had not separated by the time the gel was stopped.

The -UAA controls were designed to assess the fidelity of the translational machinery. By adding the pDULE plasmid encoding the translational machinery, but no UAA as a substrate, the machinery's specificity can be tested. If it is high fidelity, then it will not incorporate any natural amino acids and the TAG codon will be read as a stop codon by the ribosome. This will result in a truncated protein and no band at 84.2 kDa. If, on the other hand, the translational machinery is specific for the UAA's the full-length protein will be visible. It is important to note, that a band at the proper molecular weight does not tell us anything about how correctly the protein folded only that it was translated. Kinetic studies should yield more information about the protein structure. Analysis of the -UAA bands shows there is little protein present at 84.2 kDa. The contaminant bands are approximately the same size as the native and 415 mutants, so it is unlikely the -UAA cells simply expressed at a lower level. These two facts indicate the translational machinery is high fidelity.

The presence of strong bands at 84.2 kDa in the mutant cultures combined with the known fidelity of the tRNA-synthetase has significant implications for catalase research. It indicates the mutation at Tyr415 was not only successful, but resulted in accumulated protein, something that has not been achieved in literature to date.¹¹

Lastly, we can gain an idea of protein purity from the gel. There are a fair number of contaminants, but compared to the thickness of the catalase bands it can be estimated that the samples are about 80% pure catalase.

Protein yield was quantitatively assessed by UV absorbance at 595 nm (Table 3). The results support the trends seen on the gel with the 415 mutants having the highest concentration of protein, followed by the native, and then the controls. Closer inspection of protein yields reveals an interesting trend. As the size of the substituent increases and the electronegativity decreases, the yield increases. This suggests that the electronic or size properties of the Tyr415 residue may play a role in protein folding. This would be an interesting area for future catalase research.

Table 2: The absorbance at 595 nm and concentrations of the most concentrated fractions. The 415 mutants were the most concentrated followed by the native, then 206 mutants, and then the –UAA. The –UAA samples give a good idea of the degree of contamination.

Type and Fraction	Avg. Absorbance	Concentration (mg/L)
Native 1	0.647	11.77
3-Cl-Tyr415 1	0.918	15.20
3-Br-Tyr415 2	1.349	36.77
415 +pDULE –UAA 1	0.425	9.87
3-Cl-Tyr206 1	0.578	11.84
3-Br-Tyr206 2	0.504	8.98
206 +pDULE –UAA 2	0.596	13.22

Since the –UAA controls had no significant bands at 84.2 kDa, their concentration gives us a good indication of the degree of low molecular weight protein contamination in each sample (about 506 ug/mL, Table 3).

Table 3: The average absorbance of the –UAA controls was subtracted from the absorbance for each protein of interest to determine the estimate of sample purity.

	Percent Purity (assuming 506 ug/ml contamination per sample)
Native	57.1
3-Cl-Tyr415	67.0
3-Br-Tyr415	78.5

A crude activity assay was also performed (Table 4). If the catalase is active, the addition of the enzyme to H₂O₂ should generate bubbles as oxygen gas is produced. It is expected both the native and mutants will show activity. However, it is unlikely the 206 mutants will bubble since they were not designed to be functional and served only as a control for the efficacy of the translational machinery. Likewise, the –UAA samples should have resulted in a truncated protein and should not show activity. This is exactly what was found. In fact, the 415 mutants showed excellent activity, though it is important to note, they were at a much higher concentration than the native. Quantitative kinetic assays should be able to tell us more. The –UAA controls showed no activity supporting the previous data that the translational machinery is high fidelity. The 206 mutants also showed no activity supporting the hypothesis that they did not fold properly.

Table 4: The results of a crude kinetic assay. The native and 415 mutants showed excellent activity. The –UAA controls showed no activity, supporting the previous data that the translational machinery is high fidelity. The 206 mutants also showed no activity supporting the hypothesis that the Phe206 residue is important for proper folding and/or activity.

Sample	Expected Activity	Observations
Native	Yes	Bubbled
3-Cl-Tyr415	Yes	Bubbled
3-Br-Tyr415	Yes	Bubbled
415 +pDULE –UAA	No	No bubbles
3-Cl-Tyr206	No	No bubbles
3-Br-Tyr206	No	No bubbles
206 +pDULE –UAA 1	No	No bubbles

Again, the significance of these results must be emphasized. The mutant protein was not only produced, but it showed appreciable activity, going far beyond what has been achieved in literature at this site to date.¹¹

To better investigate the catalytic properties of the mutants, qualitative kinetic assays were performed. The rate of hydrogen peroxide consumption was measured by recording the pressure change as oxygen gas was produced. Based on the hypothesis, the 3-chlorotyrosine is expected to have the greatest inductive effect and thus fastest catalytic rate. The next fastest rate is predicted to be the 3-bromotyrosine mutant, followed by the native catalase.

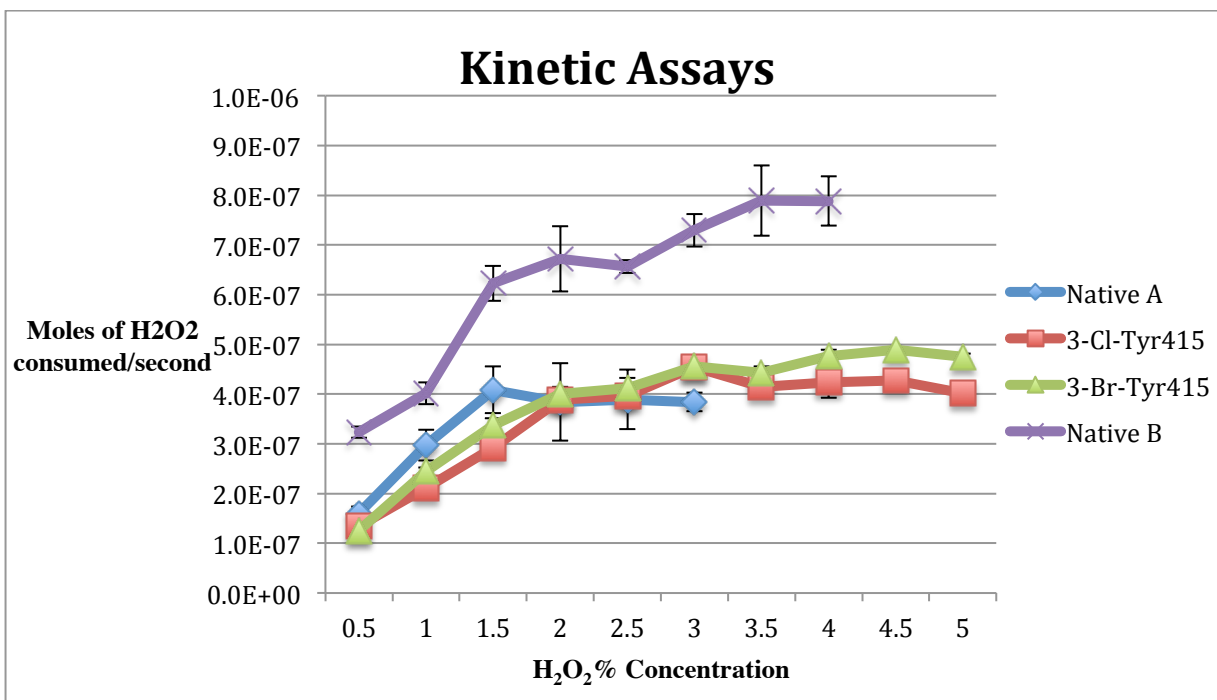


Figure 6: The rate of substrate consumption at various hydrogen peroxide concentrations. Native A used enzyme from Fraction 2, whereas Native B used enzyme from Fraction 1. The difference between fractions indicates that there is a discrepancy in regards to sample purity and differing amounts of enzyme were added. This makes a direct comparison difficult. Most importantly, the plot shows the mutants have high catalytic rates, very similar to Native A. Further kinetic tests need to be performed to determine the exact rate differences between the native and mutants.

The results of the kinetic assays were analyzed as the rate of substrate consumption at various hydrogen peroxide concentrations (Figure 6). Native A used enzyme from Fraction 2, but when that protein was depleted Native B enzyme from Fraction 1 was used. Initial results between Native A, 3-Cl-Tyr415, and 3-Br-Tyr415 showed both the mutants reaching a higher velocity than the native. However based on error bars, only one data point was significantly higher, so Native B was run at higher concentrations in order to verify the results. Since the Native B was tested two weeks after Native A, it was expected it would demonstrate a decrease in activity due to protein degradation, so the assay was run over all concentrations.

Contrary to expectations, the Native B activity was higher than Native A's. Given the small size of the error bars and the fact that Native A and B were drawn from different fractions, this result can be attributed to the amount of enzyme added. Analysis of the gels shows a fair amount of low molecular weight contaminants in the sample. The Bradford assay only relays the amount of protein in the sample and would include these contaminants. A gel was not run on native Fraction 2 due to time constraints, but it can be inferred that since the same amount of protein was added to both assays and the Native B was higher in activity than Native A, Fraction 2 must be a higher purity than Fraction 1.

The result of this is that direct comparison of the maximum velocities is not possible, but there is still useful information to be gleaned.

The first, and most significant implication of these findings is the mutants possess activity very similar to the wild type. Further kinetic tests need to be performed to determine the exact rate differences between the native and mutants, but the mere fact that these mutants had high activity holds exciting implications for understanding the role of Tyr415 in all monofunctional catalases.

The second set of useful information comes from analysis of the kinetic values (Table 5). For this analysis, traditional Michaelis-Menton assumptions are made, but it is important to note catalase HPII does not exhibit ideal Michaelis-Menton kinetics.¹¹ The values reported here are thus apparent kinetic values.

Since K_M is independent of protein concentration, it provides a useful comparison point for all samples. Analysis shows an increase in K_M in the mutants over the native. It also shows that 3-Br-Tyr415 has the highest K_M . This trend is correlated with increasing size and decreasing electronegativity of the substituent. It is not possible to ascertain which factor is contributing to the change in kinetics without further study. The higher K_m 's do indicate that the mutants require a higher concentration of substrate before they reach maximum velocity.

We also see an increase in the specificity constant as the size of the halogen increases and electronegativity decreases. Yet the turnover number is faster for 3-Br-Tyr415 and comparable to native for the 3-Cl-Tyr415. This indicates the mutants may process hydrogen peroxide faster, but with less specificity.

Table 5: Apparent kinetic values of the native catalase as compared to 3-Cl-Tyr415 and 3-Br-Tyr415 mutants. The native values are reasonable and within the same magnitude as literature. Native B results are not shown, but were within the error of Native A. Moving from native to 3-Cl-Tyr415 to 3-Br-Tyr415 a few trends emerge. The K_M increases and the specificity constant, k_{cat}/K_M decreases. These trends correlate with increasing size and decreasing electronegativity of the substituent. In addition, the turnover number for 3-Cl-Tyr415 is almost identical with that of native catalase while that of 3-Br-Tyr415 is significantly higher.

	K_M (mM)	k_{cat} (s ⁻¹) * 10 ⁴	k_{cat}/K_M (s ⁻¹ mM ⁻¹)
Native A	464 ± 211	18.7 ± 5.50	402
3-Cl-Tyr415	573 ± 85.1	17.7 ± 1.72	310
3-Br-Tyr415	832 ± 292	23.4 ± 2.53	281
Literature	220	10.1	458

Due to the issues with protein purity, there is a limit to how much useful information can be extracted about the electronic effects of the halogen substituents on the function of catalase, but this work demonstrates that such a detailed study could yield important findings.

Since the mutants had demonstrated proper folding and excellent activity, an investigation was conducted to see if the overall stability of the protein was affected by the insertion of a large halogen in the middle of the active site. The results revealed some interesting properties of the mutants (Figure 7).

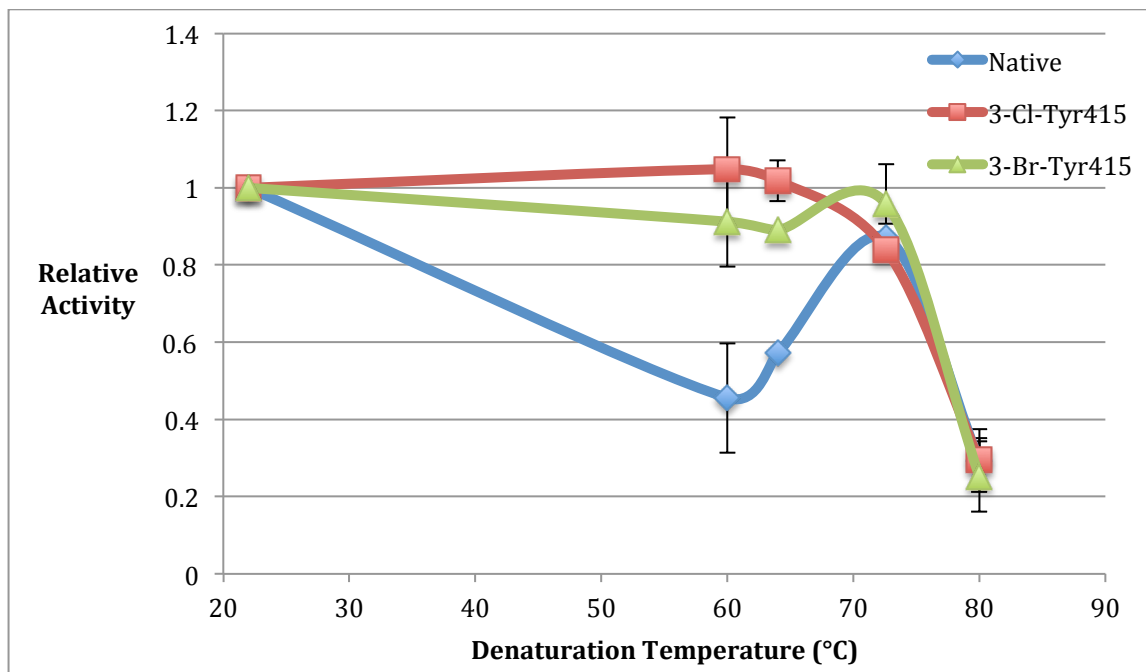


Figure 7: The results of the heat study. Relative activity is plotted as a function of denaturation temperature. Both the mutants and native lose the majority of their activity at around 80 °C. However, the mutants show a greater constancy in activity over the 22-73 °C range, indicating they are more thermostable than the native.

The first thing to note is that both the native and the mutants lose most of their activity around 80 °C. This indicates that we did not compromise the overall stability of the protein. The other observation is that the mutants demonstrate a more constant level of activity than the native over the 22-73 °C range. The mutants only lose 15% of their activity, while the native loses up to 55% of its activity. These results are surprising and the cause unclear. However, the constant activity rate of the mutants over the wide range of temperatures could be a significant benefit in industrial settings where temperature is variable but a constant kinetic output is desired. These mutants are thus more thermostable in regards to activity over the 22-73 °C range.

CONCLUSION:

The designed mutants were expressed and purified in large quantities alongside the native catalase with an approximate 67% purity for 3-Cl-Tyr-415 and 78.5% for 3-Br-Tyr-415. Quantitative kinetic assays were performed on the native catalase and 3-Cl-Tyr415 and 3-Br-Tyr415 mutants. Electronic properties were unable to be investigated due to issues with purity, but the mutants were shown to have comparable activity levels to the native. In addition, they demonstrated higher turnover numbers and lower

specificity constants as compared to native. Lastly, the mutants denatured at around the same temperature as the native but showed greater constancy in terms of activity over lower temperatures.

There are two major findings from this study. Firstly, this study showed insertion of 3-chlorotyrosine and 3-bromotyrosine at position 415 did not significantly destabilize the protein. In fact, the mutants showed greater constancy in terms of activity over a 22-73 °C range. This could have important applications in industry where temperature is variable but a constant kinetic output is desired. It also shows the tyrosyl ligand of catalases could play a role in stability.

Secondly, it demonstrated that it's not only possible to alter the proximal ligand of the heme group, but protein can be accumulated in significant amounts with activity levels similar to native catalase HP11. This has never been done before in literature and possesses serious implications for the ability of scientists to understand the catalytic role of the tyrosine ligand in monofunctional catalases.

REFERENCES:

1. Obinger, C., Maj, M., Nicholls, P. & Loewen, P. Activity, Peroxide Compound Formation, and Heme d Synthesis in *Escherichia coli* HPII Catalase. *Arch. Biochem. Biophys.* **342**, 58–67 (1997).
2. Chelikani, P., Fita, I. & Loewen, P. C. Diversity of structures and properties among catalases. *Cell. Mol. Life Sci. CMLS* **61**, 192–208 (2004).
3. Zamocky, M., Furtmüller, P. G. & Obinger, C. Evolution of Catalases from Bacteria to Humans. *Antioxid. Redox Signal.* **10**, 1527–1548 (2008).
4. Maté, M. J. *et al.* in *Handbook of Metalloproteins* (John Wiley & Sons, Ltd, 2006).
5. Cutler, R. G. Oxidative stress and aging: catalase is a longevity determinant enzyme. *Rejuvenation Res.* **8**, 138–140 (2005).
6. Milano, A. *et al.* The *katE* gene, which encodes the catalase HPII of *Mycobacterium avium*. *Mol. Microbiol.* **19**, 113–123 (1996).
7. Melik-Adamyany, W. *et al.* Substrate flow in catalases deduced from the crystal structures of active site variants of HPII from *Escherichia coli*. *Proteins* **44**, 270–281 (2001).
8. Jha, V. *et al.* Modulation of Heme Orientation and Binding by a Single Residue in Catalase HPII of *Escherichia coli*. *Biochemistry (Mosc.)* **50**, 2101–2110 (2011).
9. Alfonso-Prieto, M., Vidossich, P. & Rovira, C. The reaction mechanisms of heme catalases: An atomistic view by ab initio molecular dynamics. *Arch. Biochem. Biophys.* **525**, 121–130 (2012).
10. de Visser, S. P. What External Perturbations Influence the Electronic Properties of Catalase Compound I? *Inorg. Chem.* **45**, 9551–9557 (2006).

11. Loewen, P. Probing the structure of catalase HPII of *Escherichia coli*--a review. *Gene* **179**, 39–44 (1996).
12. Yu, Y. *et al.* Defining the Role of Tyrosine and Rational Tuning of Oxidase Activity by Genetic Incorporation of Unnatural Tyrosine Analogs. *J. Am. Chem. Soc.* **137**, 4594–4597 (2015).
13. Kari Van Zee, Ryan Mehl. BB 494 Laboratory Manual.
14. Louis, S. *The Role of Key Residues in the Lateral Channel of the E. Coli Catalase HPII [microform]*. (Thesis (M.Sc.)--University of Manitoba, 2004).

SUPPLEMENTAL:

Table S1: Components of autoinduction media. Designed so that arabinose induces expression during the exponential growth phase for a 1:100 cell dilution in 75 mL of media.

Aspartate (5%, pH 7.5)	12.5 mL
Glycerol (10%)	12.5 mL
25x Mineral Salts	10.0 mL
Glucose (40%)	0.3125 mL
MgSO ₄ (1M)	0.5 mL
Arabinose (20%)	0.625 mL
Trace Metals (5000x)	0.05 mL
18 AA Mix (25x)	10.0 mL
Ampicillin (100ug/uL)	0.250 mL
Sterile Water	To final volume of 250 mL (203.2 mL)

Table S2: The compositions of all buffers used

Equilibration Buffer (5X)	250 mM sodium phosphate, 1.5 M NaCl pH 7.0
Elution Buffer	50 mM sodium phosphate, 300 mM NaCl, 250 mM imidazole, pH 7.0
Sodium Phosphate Buffer	0.1M, pH 7.0
SDS-PAGE Running Buffer (10X)	125 mM Tris base, 960 mM glycine, and 0.5% SDS in DI H ₂ O, pH8.3

Table S3: Absorbance at 595 nm of all protein fractions using UV-Vis spectrophotometer

Type and fraction	1	2	3	avg	Concentration (ug/ml)
wt 1	0.666	0.654	0.622	0.647	672.66
wt 2	0.497	0.456	0.442	0.465	463.74
wt 3	0.021	0.025	0.025	0.024	23.52
wt 4	0.009	0.009	0.008	0.009	9.81
Cl 415 1	0.97	0.921	0.864	0.918	1029.44
Cl 415 2	0.256	0.256	0.252	0.255	244.27
Cl 415 3	0.003	0.008	0.008	0.006	7.68
Cl 415 4	0.019	0.02	0.018	0.019	19.25
415 -UAA 1	0.005	0.003	0.002	0.003	4.94
415 -UAA 2	0.431	0.426	0.419	0.425	420.77
415 -UAA 3	0.178	0.177	0.197	0.184	174.73
415 -UAA 4	0.023	0.024	0.025	0.024	23.83
Br 415 1	0.032	0.031	0.03	0.031	30.26
Br 415 2	1.419	1.366	1.262	1.349	1851.67
Br 415 3	0.423	0.402	0.391	0.405	399.40
Br 415 4	0.045	0.046	0.051	0.047	45.31
Cl 206 1	0.576	0.573	0.586	0.578	591.22
Cl 206 2	0.146	0.156	0.175	0.159	150.58
Cl 206 3	-0.007	-0.003	-0.001	-0.004	-1.42
Cl 206 4	-0.012	-0.012	-0.015	-0.013	-9.89
206 -UAA 1	0.211	0.212	0.227	0.217	206.64
206 -UAA 2	0.602	0.601	0.585	0.596	611.78
206 -UAA 3	0.298	0.298	0.32	0.305	295.34
206 -UAA 4	0	0.006	0.008	0.005	6.16
Br 206 1	0.495	0.496	0.522	0.504	507.16
Br 206 2	0.064	0.066	0.065	0.065	61.69
Br 206 3	-0.005	-0.004	-0.007	-0.005	-2.94

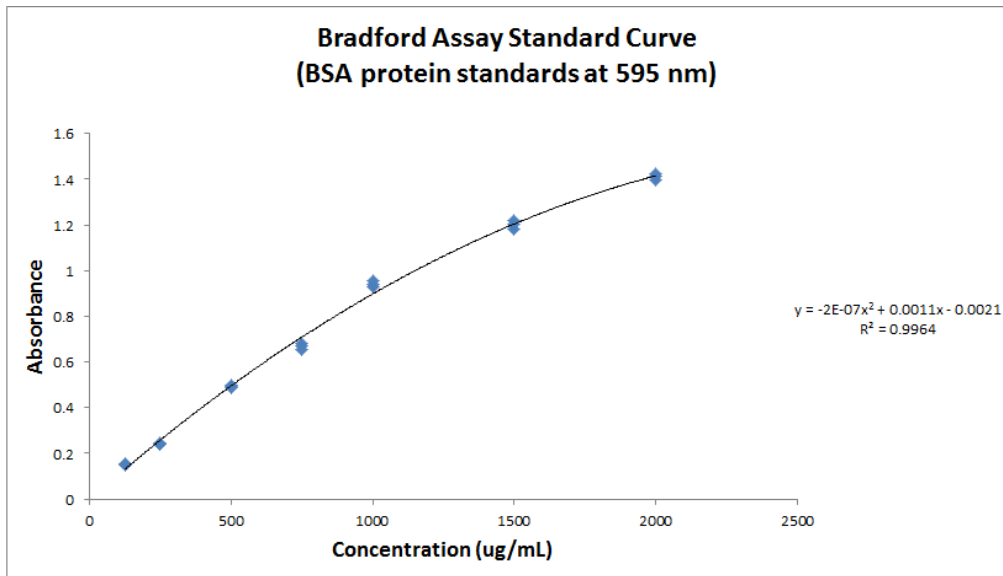


Figure S1: The standard Bradford Assay curve used to determine concentrations of purified proteins.

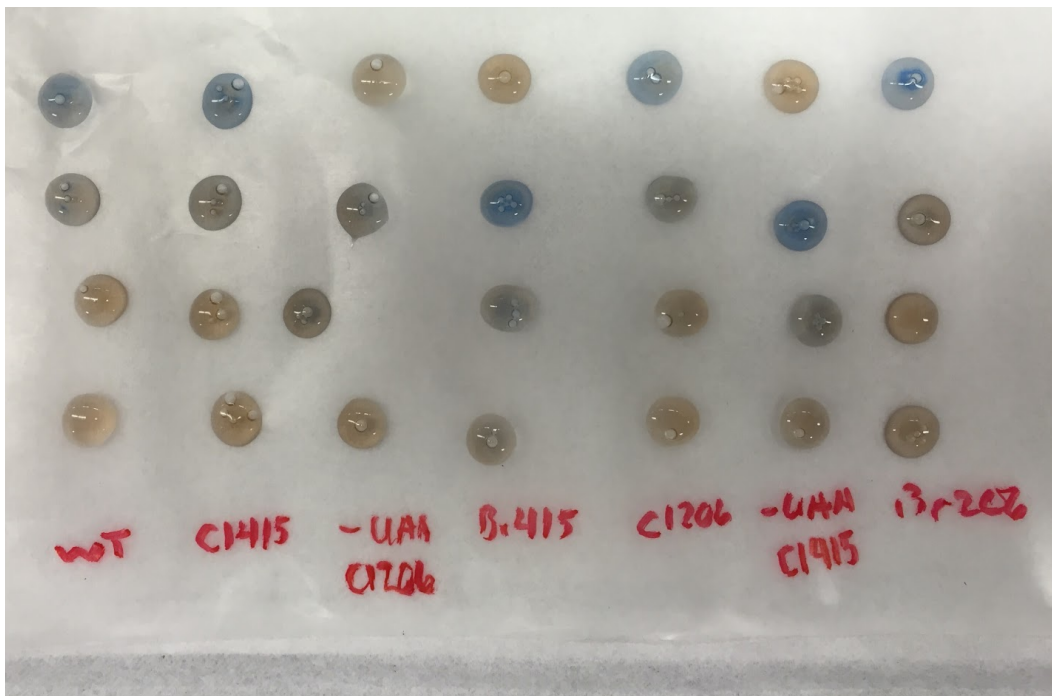


Figure S2: The qualitative Bradford assay showing protein (blue) in at least one fraction of every protein type.